Chapter 9
Test-to-Failure Characterization and Acceleration Signal Feature Analysis of Electronic Systems Under Repeated Shock Loading

Trotter Roberts, Hugo Luck, Joud N. Satme, Mohsen Gol Zardian, Sina Navidi, Ryan Yount, Austin R.J. Downey, and Chao Hu

Abstract Electronic systems operating in high-rate dynamic environments are susceptible to mechanical and electrical failure due to extreme shock loading. Understanding how shock response correlates with physical degradation in electronic components is critical for predicting failure and designing more resilient hardware or active control solutions. This study presents a repeatable testing framework for evaluating damage accumulation in printed circuit boards (PCBs) subjected to high-energy shock events. In this work, a PCB with an onboard resistor is mounted as a fixed-fixed beam and exposed to a test-to-failure sequence under a constant shock energy profile. High-resolution electrical resistance is monitored in situ over the course of each test to track the initiation and evolution of damage. Simultaneously, high-speed acceleration data is collected via PCB-mounted sensors, enabling detailed analysis of dynamic system behavior under repeated mechanical loading. By applying this protocol across multiple boards of identical configuration, the study generates a consistent and controlled dataset for assessing how dynamic response features relate to damage progression in electronics subjected to shock events. A series of time- and frequency-domain features (e.g., root-mean-square amplitudes, crest factors, and spectral centroids) are extracted from the acceleration signals. These features are then analyzed alongside resistance trends to identify consistent markers that precede or coincide with failure. While no online learning algorithms are implemented in this study, the framework is explicitly designed to support the development and evaluation of real-time machine learning-based classifiers for electronic condition assessment in high-rate environments, including potential applications in onboard sensing, autonomous fault detection, and predictive maintenance of mission-critical systems. All data is shared through a public repository.

Keywords Structural health monitoring · Damage detection · Feature extraction · Shock testing · Reliability

Introduction

In many high-performance applications, electronic hardware is subjected to intense shock events that can rapidly degrade structural and electrical integrity. Shock events are high-energy impulses occurring within microseconds to milliseconds, generate enormous stress gradients and abrupt deformations that threaten the integrity of mission-critical electronics. Conventional structural health monitoring and fatigue assessment techniques struggle to operate within these severe time constraints, where damage can accumulate before diagnostic systems can react [1]. Passive design techniques, like shock-

Trotter Roberts · Hugo Luck · Joud N. Satme · Mohsen Gol Zardian · Ryan Yount · Austin R.J. Downey
Department of Mechanical Engineering, University of South Carolina, Columbia, SC 29208
e-mail: tjr7@email.sc.edu; golzardm@email.sc.edu; jsatme@email.sc.edu; golzardm@email.sc.edu; rjyount@email.sc.edu; austindowney@sc.edu

Sina Navidi · Chao Hu
School of Mechanical, Aerospace, and Manufacturing, University of Connecticut, Storrs, CT 06269
e-mail: sina.navidi@uconn.edu; chao.hu@uconn.edu

Austin R.J. Downey
Department of Civil and Environmental Engineering, University of South Carolina, Columbia, SC 29208
e-mail: austindowney@sc.edu

© The Author(s), under exclusive license to River Publishers 2026

Kristin B. Zimmerman, PhD (eds.), *Dynamic Evironments and Durability Testing, 2026, Vol. 7*, Conference Proceedings of the Society for Experimental Mechanics Series, https://doi.org/10.13052/rp-9788743814184

absorbing mounts or ruggedized enclosures, offer some protection but are unable to completely reduce failure risks when repeated shock loads cause progressive damage to delicate components [2].

To address the reliability limitations of electronics subjected to shock, there is an increasing need for high-fidelity testing and monitoring frameworks that link dynamic shock response features to physical damage evolution in electronic hardware. Prior studies have demonstrated the value of vibration and shock testing for mechanical assemblies [3], but electronic systems introduce additional complexities arising from the coupled mechanical–electrical failure modes of printed circuit boards. printed circuit boards (PCBs) damage frequently starts as trace delamination or microcracking in solder joints, which can show up as minor variations in electrical resistance prior to catastrophic failure [4]. Understanding how particular loading conditions accelerate damage requires robust analysis of time- and frequency-domain dynamic features in conjunction with in situ sensing at high temporal resolution in order to capture these early-stage signatures [5].

Active monitoring during controlled laboratory shock experiments provides a pathway to generate repeatable, high-rate datasets that reveal the interplay between mechanical response and electronic degradation. By mounting PCBs as structural elements, such as fixed-fixed beams, test configurations can reproduce realistic boundary conditions and load transfer pathways seen in embedded electronic assemblies [6]. When paired with high-speed acceleration sensing, this approach enables simultaneous observation of both the system's dynamic behavior and the onset of electrical performance degradation. Extracting statistical and spectral features from the shock response, such as root-mean-square amplitudes, crest factors, and spectral centroids, can yield early indicators of cumulative damage prior to failure [7].

This study introduces a repeatable shock testing framework to evaluate damage accumulation in PCBs subjected to controlled high-energy impact sequences. All data is shared through a public repository [8]. Electrical resistance is monitored in situ throughout the test-to-failure process, while high-speed acceleration data is simultaneously recorded to capture the dynamic response. By applying an identical test protocol across multiple boards, the framework produces a consistent dataset that links time- and frequency-domain shock response features to progressive electrical degradation. Although no learning algorithms are implemented here, the experimental design explicitly supports future integration of machine learning-based classifiers for real-time fault detection and predictive maintenance in high-rate operational environments. The primary contributions of this work are twofold. First, it provides a controlled experimental platform for quantifying the relationship between high-rate shock response features and progressive electrical failure in PCBs. Second, it establishes a feature extraction methodology and cumulative damage framework that lays the groundwork for future real-time, learning-enabled monitoring of electronic systems in extreme dynamic environments.

Background

Controlled laboratory shock environments are commonly used to replicate the transient loading conditions found in operational platforms to study these effects. Drop towers, pneumatic impactors, and similar setups allow researchers to apply repeatable, high-energy impulses to test specimens while controlling boundary conditions and impact energy. Fixed–fixed or cantilever mounting arrangements are frequently used because they reproduce realistic load transfer paths and constraint conditions seen in embedded assemblies [9]. Such controlled test environments have been shown to isolate specific failure mechanisms, making it possible to correlate the PCB's structural response with progressive electrical damage [10]. Time-domain features such as root-mean-square (RMS) acceleration, crest factor, and signal energy ratios can capture changes in amplitude and impulse response. Likewise, frequency-domain features, including spectral centroid shifts and energy redistribution across frequency bands, can reveal subtle structural softening or nonlinear effects that occur as damage accumulates [11]. In our specific application, these features provide a way to quantify subtle changes in response behavior that may correlate with solder joint fatigue or progressive micro-cracking.

Methodology

PCBs fabricated from FR4 were prepared as test specimens. Each board measured 25.40 mm $\times$ 76.20 mm $\times$ 1.60 mm and contained a single 100 mΩ, 1 W surface-mount resistor soldered at midspan using a controlled stencil process to reduce variability. The boards were mounted as fixed–fixed beams in a custom aluminum fixture (Figure 1), providing rigid boundary conditions representative of embedded electronic assemblies.

Shock loading was applied using a drop tower system (Figure 2), where a guided mass was released from a height of 12 inches (0.305 m), producing repeatable shock pulses of approximately 5000 g. The drop height and mass were held constant across all tests to ensure consistent impact energy. Dynamic response was measured using Endevco 727 piezoresis-

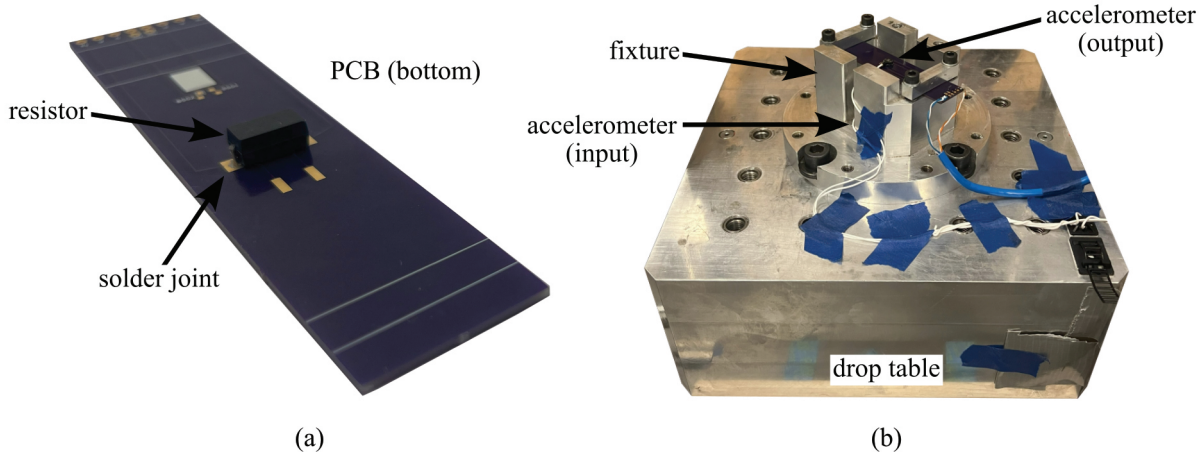


Fig. 1 The considered test setup, showing: (a) PCBs specimen with a surface-mount resistor attached at midspan (bottom side up), and (b) PCB mounted in the aluminum fixture in a fixed–fixed configuration.

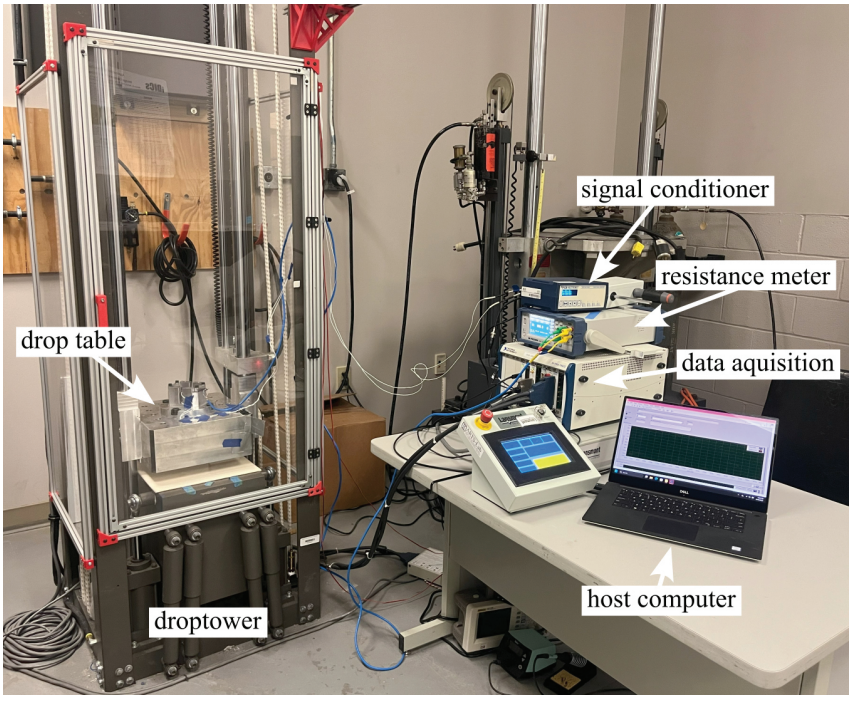


Fig. 2 The experimental setup for repeated shock testing.

tive accelerometers (20k g range, DC–50 kHz bandwidth). One accelerometer was mounted on the fixture beneath the PCB midspan to capture input excitation, while another was placed at the PCB surface at midspan to record local response. Acceleration signals were conditioned with a PCB 482C unit (gain 100×) and digitized using a PXIe-4483 module at 200 kHz, yielding 20,000 samples over a 0.1 s window per shock event. A representative excitation–response time history is shown in Figure 3.

Electrical resistance was monitored in situ with a BK Precision 2841 micro-ohmmeter (0.1 $\mu\Omega$ resolution, 0.01% accuracy) in a four-wire configuration to minimize lead effects. After each impact, ten consecutive resistance readings were recorded and averaged to provide one value per event. Acceleration and resistance data were acquired simultaneously, enabling direct correlation between mechanical response and electrical degradation. A total of ten boards were tested under identical conditions. Each was subjected to repeated shocks until failure, defined as an irreversible increase in resistance

beyond baseline variability. All boards were tested to failure, and three representative cases are reported here for clarity and consistency.

Following data collection, acceleration and resistance signals were processed to extract features representative of system dynamics and progressive damage. Time-domain features included maximum amplitude, root-mean-square (RMS) value, absolute mean, skewness, kurtosis, crest factor, shape factor, and impulse factor. Frequency-domain features such as spectral centroid and bandwidth were also calculated. To allow direct comparison across boards and impact histories, all features were normalized with respect to their initial values.

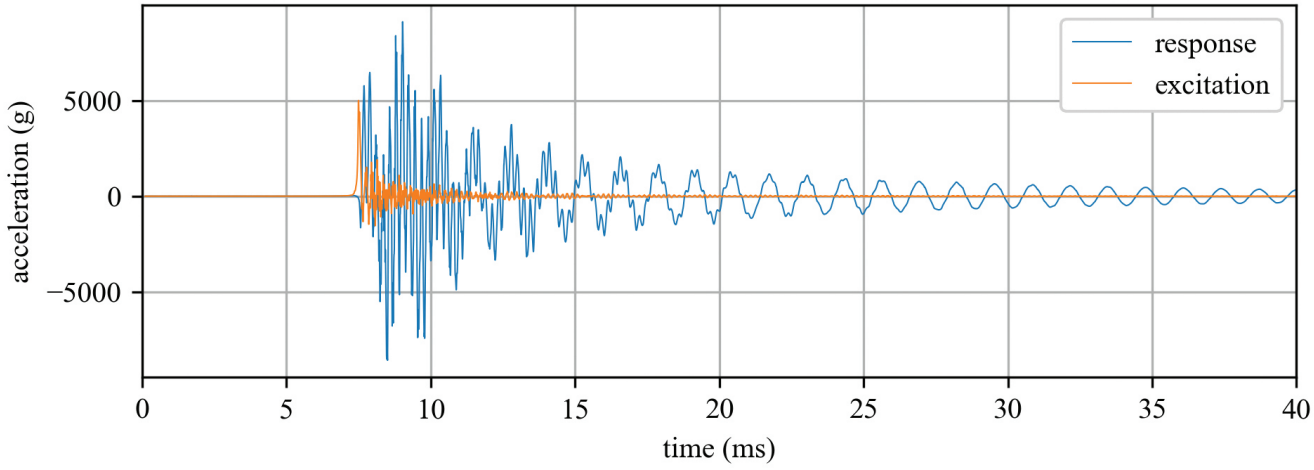


Fig. 3 Excitation and response acceleration time series under repeated impact.

Results and Analysis

The resistance histories of all three representative test boards are presented in Figure 4. These plots show the evolution of electrical resistance over the course of repeated impacts, providing a direct view of how each board progressed to failure. Although the number of shocks sustained and the absolute resistance values at failure varied between boards, a common pattern emerged. After an initial break-in period, resistance typically increased sharply, then transitioned to a slower, more gradual rise before the onset of failure. Outliers were observed where resistance deviated from this general progression, highlighting the inherent variability in solder joint and trace degradation.

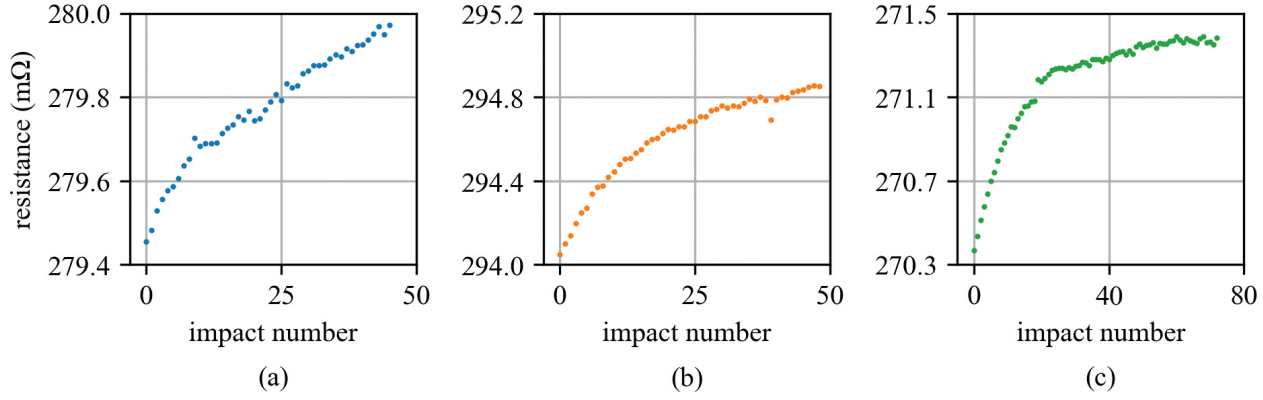


Fig. 4 Raw resistance versus impact number for (a) board 1, (b) board 2, and (c) board 3.

To better illustrate consistent resistance degradation trends, Figure 5 presents resistance histories after manual preprocessing. Outliers were first removed, followed by trimming the initial break-in period and the final few impacts where failure

was imminent. While these segments are excluded here for clarity, the complete datasets remain available in the shared repository for future analysis [8]. As shown, the processed resistance measurements reveal a common progression across boards: gradual drift followed by abrupt increases approaching failure. Figure 5 also includes fitted exponential trend-lines of the form

$$y(x) = \frac{100\left(1 - e^{-bx}\right)}{1 - e^{-100b}}, \tag{1}$$

where x is the normalized impact number (0–100), y is the normalized resistance (0–100), and b is a fitted growth-rate parameter. The anchoring ensures that all curves pass exactly through $(0, 0)$ and $(100, 100)$, enabling direct comparison between boards. The fitting was performed using nonlinear least-squares optimization via the `curve_fit` function from the `SciPy` library [12].

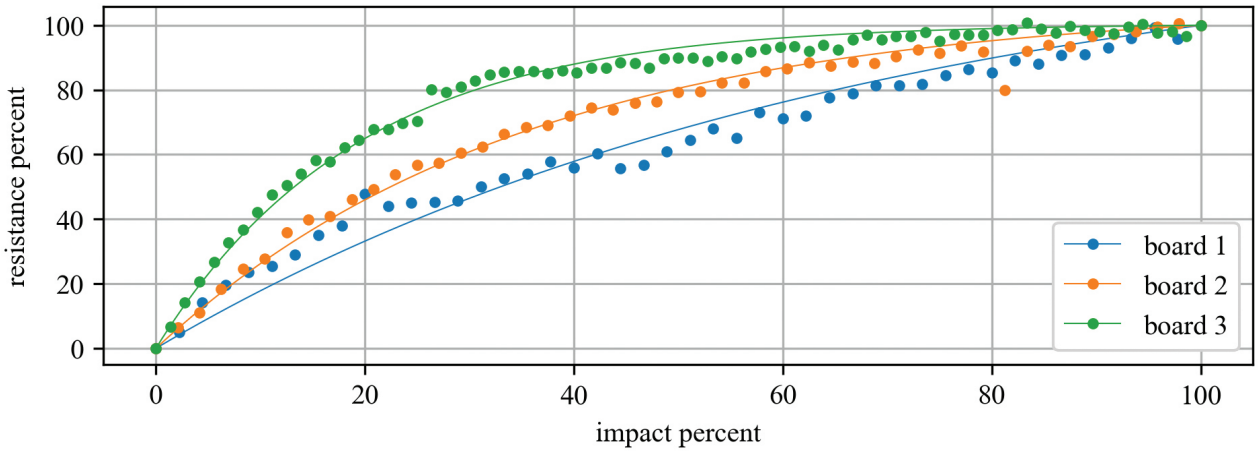


Fig. 5 Normalized resistance versus impact number with superimposed exponential trendline fits for selected boards.

Dynamic response features derived from acceleration data were analyzed in the time domain. Figures 6–8 illustrate the evolution of normalized features across repeated impacts for three representative boards. For Board 1, shape factor, RMS,

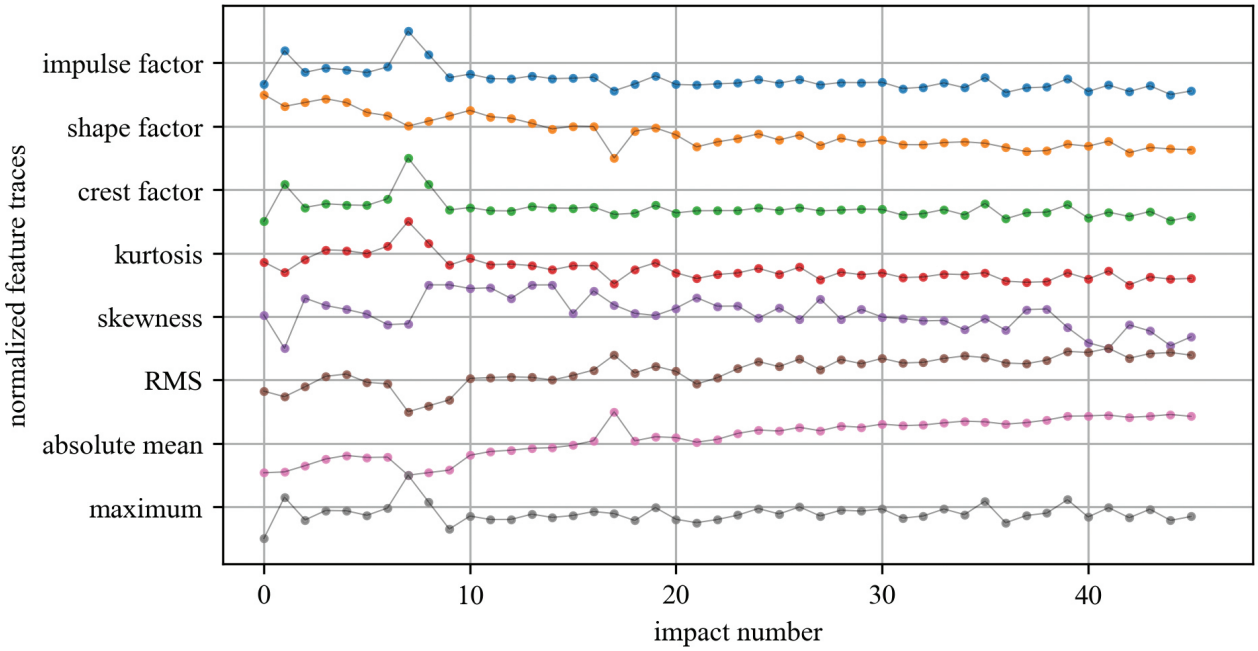


Fig. 6 Normalized time-domain features extracted from excitation and response signals for Board 1.

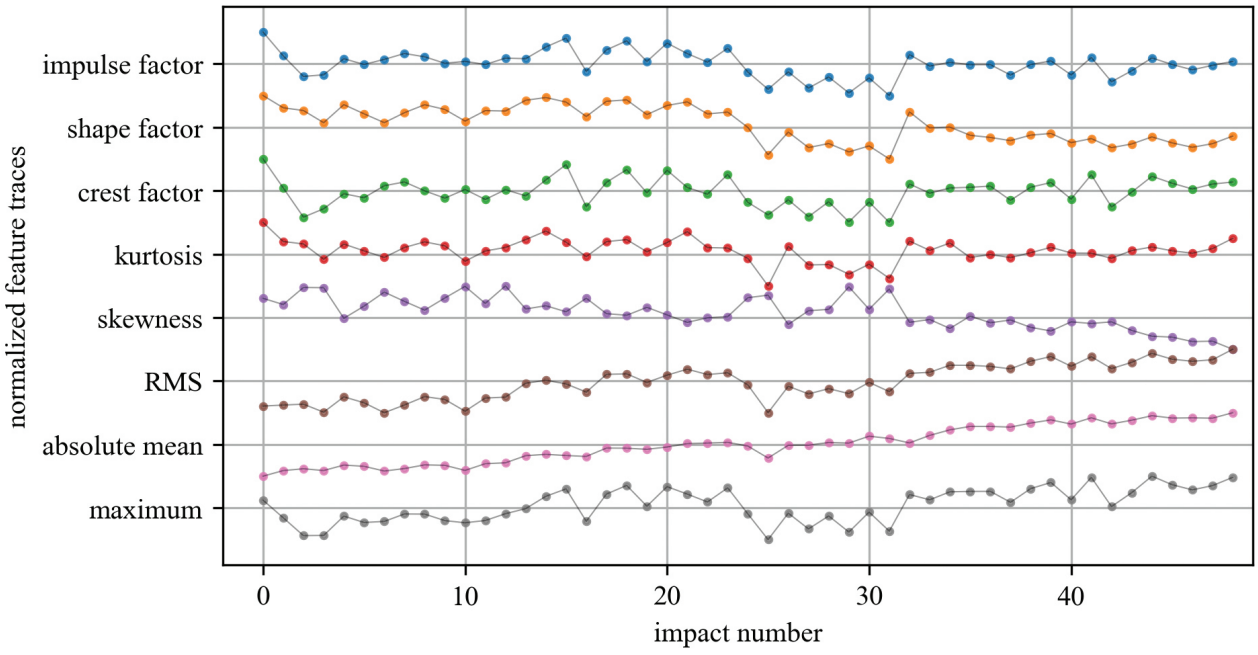


Fig. 7 Normalized time-domain features extracted from excitation and response signals for Board 2.

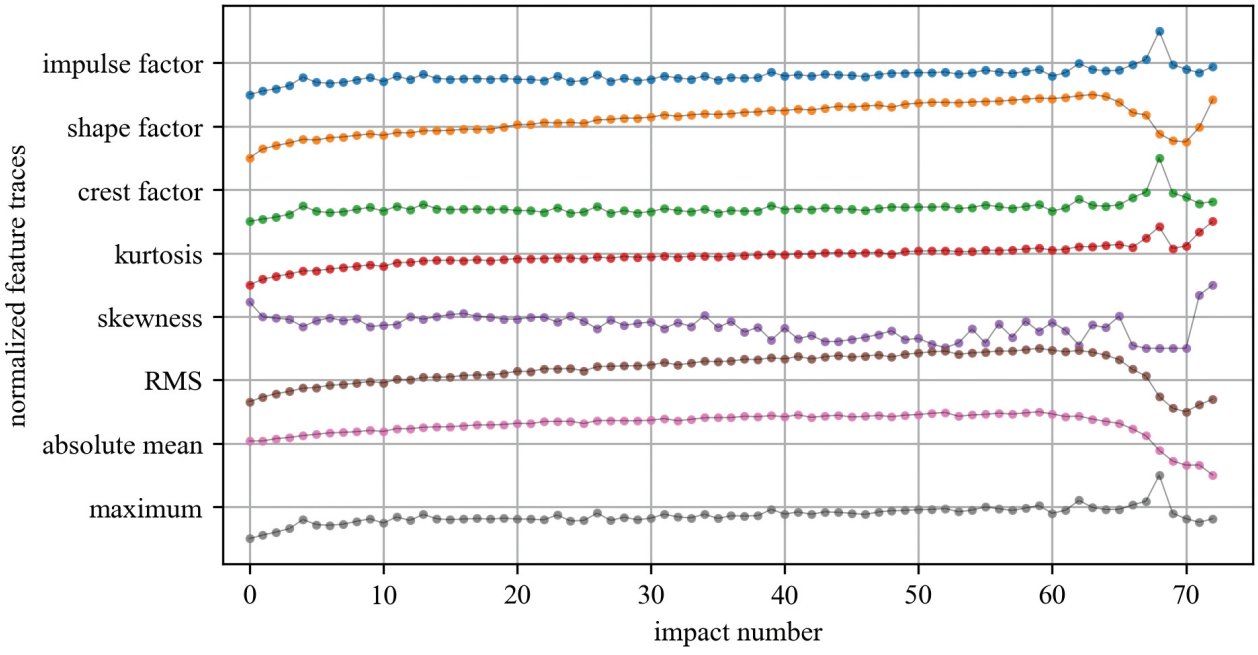


Fig. 8 Normalized time-domain features extracted from excitation and response signals for Board 3.

and absolute mean showed gradual upward trends, while the other features remained relatively stable throughout most of the sequence. Board 2 exhibited similar behavior, with RMS and absolute mean sharing consistent visible trends, while crest factor and kurtosis remained essentially flat; this board also displayed the highest variability in individual data points, suggesting greater issues in data collection, something expected as measuring high-rate impact events is experimentally challenging to do without noise. Board 3 displayed the clearest late-stage excursions: although all features followed steady trends through most of the test, shape factor, RMS, and absolute mean dropped sharply during the last 10–15 impacts

following steady climbs, coinciding with the abrupt resistance increase near failure. These observations indicate that while some features provide gradual indicators of cumulative degradation, others remain stable until close to failure, where rapid excursions reveal the onset of irreversible damage.

The Pearson correlation coefficient r quantifies the strength and direction of a linear relationship between the fitted resistance degradation trendline and each feature trajectory [13]. Values of r range from -1 (perfect negative correlation) to $+1$ (perfect positive correlation), with values near zero indicating little to no linear association. The associated p-value tests the null hypothesis of no correlation, with $p < 0.05$ taken as statistically significant. Because Pearson correlation is limited to linear trends, the Spearman rank correlation coefficient ρ was also evaluated. Spearman correlation measures monotonic associations, making it more robust in cases where feature trajectories evolve nonlinearly with degradation [14, 15]. Tables 1 and 2 summarize both correlation metrics across the three boards, with the final column reporting the mean $\pm$ standard deviation.

The results show clear differences between the two measures. Features such as *absolute mean* and *RMS* yielded moderate Pearson correlations ($r \approx 0.5$) but much higher Spearman values ($\rho > 0.75$), suggesting strong but nonlinear monotonic relationships with resistance. Conversely, *kurtosis* and *skewness* displayed inconsistent Pearson values, including negative correlations, yet ranked among the strongest features under Spearman analysis, reflecting late-stage nonlinear excursions near failure. In contrast, features like *crest factor* and *shape factor* remained weak under both measures. Overall, *absolute mean*, *RMS*, and *kurtosis* emerged as the most reliable indicators of cumulative degradation across boards. These results are visualized in Figure 9, where features are ranked by mean absolute importance to emphasize the most informative indicators of cumulative damage progression.

Table 1 Pearson correlation results for boards 1–3, with mean correlation across boards.

	board 1		board 2		board 3		mean $\pm$ std
feature	r	p-value	r	p-value	r	p-value	r
impulse factor	-0.272	6.77×10^{-2}	-0.329	2.09×10^{-2}	0.263	2.44×10^{-2}	-0.113 ± 0.327
shape factor	-0.397	6.29×10^{-3}	-0.673	1.20×10^{-7}	0.198	9.39×10^{-2}	-0.291 ± 0.445
crest factor	-0.265	7.51×10^{-2}	-0.041	7.82×10^{-1}	0.174	1.41×10^{-1}	-0.044 ± 0.220
kurtosis	-0.222	1.38×10^{-1}	-0.322	2.39×10^{-2}	0.579	7.85×10^{-8}	0.012 ± 0.494
skewness	-0.182	2.27×10^{-1}	-0.634	1.02×10^{-6}	-0.309	7.82×10^{-3}	-0.375 ± 0.233
RMS	0.529	1.56×10^{-4}	0.801	4.98×10^{-12}	0.207	7.96×10^{-2}	0.512 ± 0.297
absolute mean	0.555	6.19×10^{-5}	0.907	3.17×10^{-19}	0.103	3.85×10^{-1}	0.522 ± 0.403
maximum	-0.137	3.65×10^{-1}	0.525	1.08×10^{-4}	0.634	1.72×10^{-9}	0.341 ± 0.417

Table 2 Spearman correlation results for boards 1–3, with mean correlation across boards.

	board 1		board 2		board 3		mean $\pm$ std
feature	ρ	p-value	ρ	p-value	ρ	p-value	ρ
impulse factor	-0.771	3.58×10^{-10}	-0.353	1.28×10^{-2}	0.820	7.04×10^{-19}	-0.101 ± 0.825
shape factor	-0.883	4.79×10^{-16}	-0.728	3.16×10^{-9}	0.684	2.67×10^{-11}	-0.309 ± 0.863
crest factor	-0.554	6.55×10^{-5}	0.072	6.23×10^{-1}	0.609	1.11×10^{-8}	0.042 ± 0.582
kurtosis	-0.786	1.02×10^{-10}	-0.266	6.50×10^{-2}	0.940	6.63×10^{-35}	-0.037 ± 0.885
skewness	-0.555	6.23×10^{-5}	-0.758	2.86×10^{-10}	-0.571	1.33×10^{-7}	-0.628 ± 0.113
RMS	0.873	2.56×10^{-15}	0.868	7.21×10^{-16}	0.530	1.39×10^{-6}	0.757 ± 0.196
absolute mean	0.929	1.37×10^{-20}	0.974	6.52×10^{-32}	0.416	2.55×10^{-4}	0.773 ± 0.310
maximum	0.020	8.95×10^{-1}	0.612	2.97×10^{-6}	0.729	2.50×10^{-13}	0.454 ± 0.380

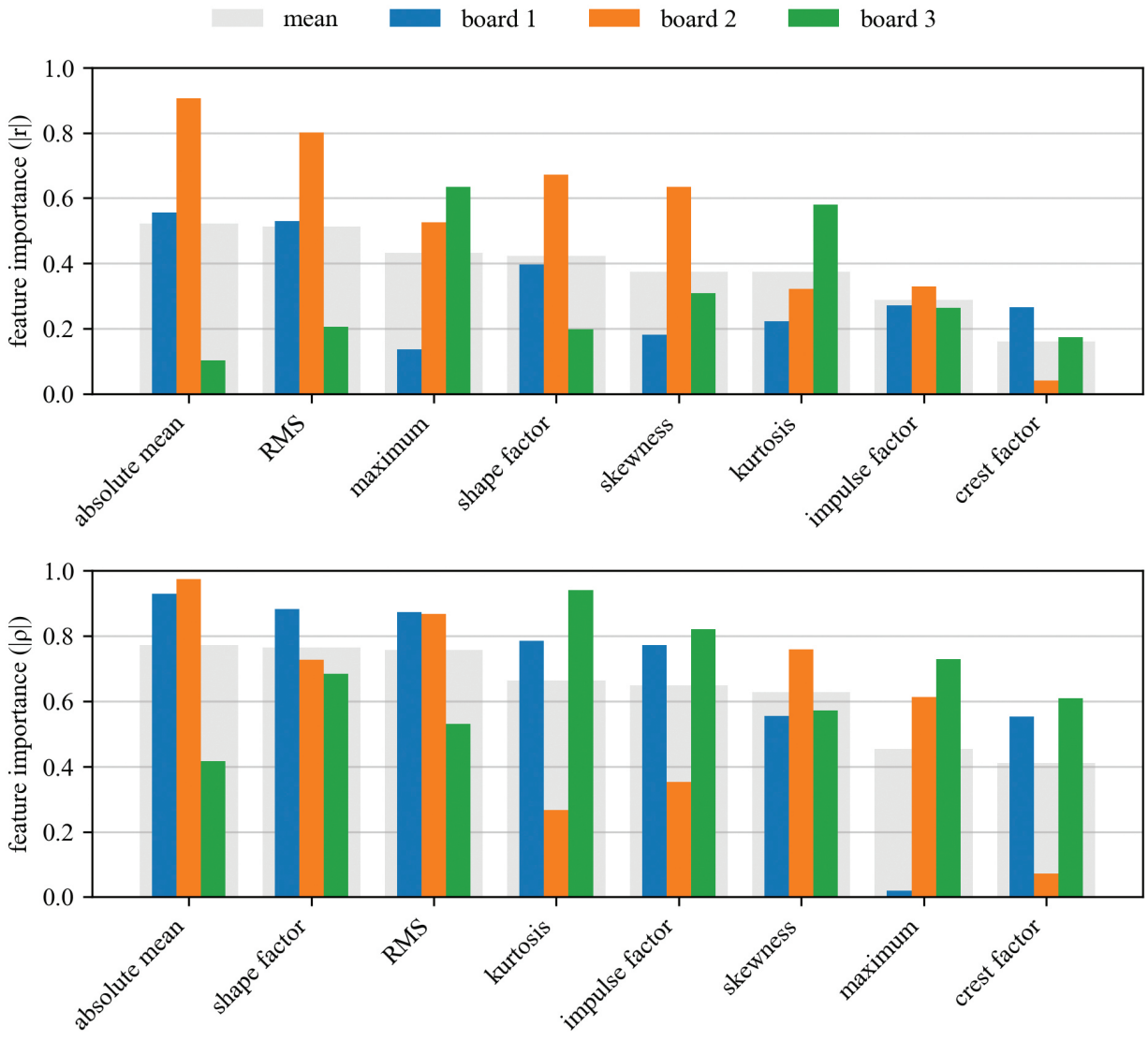


Fig. 9 Feature importance based on absolute mean correlation across boards, shown for both Pearson (top) and Spearman (bottom).

Conclusion

This study introduced a repeatable experimental framework for evaluating cumulative damage in PCBs subjected to repeated high-g shock events. The framework created a controlled dataset that connected dynamic response features to progressive electrical degradation by fusing high-rate acceleration measurements along with resistance monitoring. Resistance histories consistently exhibited gradual drift followed by abrupt increases prior to failure, while feature trajectories revealed both steady long-term trends and late-stage excursions. Correlation analysis identified maximum, kurtosis, and skewness as the most reliable indicators of degradation, highlighting their potential value for monitoring cumulative damage in high-rate environments. Overall, the results establish initial links between mechanical shock response and electrical degradation in PCBs.

By quantifying feature–damage correlations and demonstrating the reproducibility of the experimental protocol, this study establishes the foundation for condition indicators that can aid in real-time failure diagnosis. In the future, the framework will be expanded to include more PCB shapes and loading scenarios, incorporate cumulative damage data more clearly, and use machine learning techniques for predictive maintenance and categorization. When combined, these advancements

will make it possible to use more reliable, data-driven methods to guarantee the dependability of electronics used in extremely dynamic settings.

Acknowledgments This material is based upon work supported by the National Science Foundation grant numbers CCF - 1956071, CCF-2234921, and CPS - 2237696. Additional support was provided from the Air Force Office of Scientific Research (AFOSR) through award no. FA9550-21-1-0083. Any opinions, findings conclusions, or recommendations expressed in this material are those of the authors and do not necessarily reflect the views of the National Science Foundation or the United States Air Force.

References

1. Dodson, J., Downey, A., Laflamme, S., Todd, M.D., Moura, A.G., Wang, Y., Mao, Z., Avitabile, P., and Blasch, E. "High-rate structural health monitoring and prognostics: An overview". In *Data Science in Engineering, Volume 9*, pages 213–217. Springer International Publishing (2021)ifnextchar.gobble.
2. Fisco, N. and Adeli, H. "Smart structures: Part i—active and semi-active control". *Scientia Iranica*, 18(3):275–284 (2011)ifnextchar.gobble.
3. Roberts, T., Yount, R., Dodson, J., Moura, A., and Downey, A.R. "Towards active structural control strategies for electronic assemblies in high-rate dynamic environments.". SAVE, 94th Shock and Vibration Symposium (2024)ifnextchar.gobble.
4. Hu, B., Sun, Y., and Wu, S. "Vibration characteristics and lead stress optimization for printed circuit board with pqfp under random loads". *Microelectronics Reliability*, 171:115817 (2025)ifnextchar.gobble.
5. Buckley, T., Ghosh, B., and Pakrashi, V. "A feature extraction & selection benchmark for structural health monitoring". *Structural Health Monitoring*, 22(3):2082–2127 (2022)ifnextchar.gobble.
6. Yount, R., Roberts, T., Dodson, J., Moura, A., and Downey, A.R. "Experimental analysis to enable low-latency structural health monitoring for electronics in high-rate dynamic environments". Springer Nature Switzerland (2025)ifnextchar.gobble.
7. Satme, J.N., Coble, D., and Downey, A.R.J. "Online health monitoring of electronic components subjected to repeated high-energy shock". In *ASME 2024 Conference on Smart Materials, Adaptive Structures and Intelligent Systems*, SMASIS2024. American Society of Mechanical Engineers (2024)ifnextchar.gobble.
8. ARTS-Lab. "Paper-2026-test-to-failure-characterization". GitHub (2026)ifnextchar.gobble. https://github.com/ARTS-Laboratory/Paper-2026-Test-to-Failure-Characterization.
9. Roberts, T., Gol Zardian, M., Satme, J.N., and Downey, A.R.J. "Finite element modeling of fixed-fixed beams under shock excitation with active control". IMECE, American Society of Mechanical Engineers (2025)ifnextchar.gobble.
10. Muthuram, N. and Saravanan, S. "Fatigue life based study of electronic package mounting locations on printed circuit boards subjected to random vibration loads". *Journal of Electronic Testing*, 40(6):761–776 (2024)ifnextchar.gobble.
11. Liu, F., Gong, R., Duan, Z., Wang, Z., and Zhou, J. "Research on vibration reliability of solder joint based on modal experiment of pcba". *Journal of Materials Science: Materials in Electronics*, 36(1) (2024)ifnextchar.gobble.
12. Virtanen, P., Gommers, R., Oliphant, T.E., and et al. "Scipy 1.0: fundamental algorithms for scientific computing in python". *Nature Methods*, 17(3):261–272 (2020)ifnextchar.gobble.
13. Pearson, K. "Vii. note on regression and inheritance in the case of two parents". *Proceedings of the Royal Society of London*, 58(347–352):240–242 (1895)ifnextchar.gobble.
14. Spearman, C. "The proof and measurement of association between two things". *The American Journal of Psychology*, 100(3/4):441 (1987)ifnextchar.gobble.
15. Hauke, J. and Kossowski, T. "Comparison of values of pearson's and spearman's correlation coefficients on the same sets of data". *QUAGEO*, 30(2):87–93 (2011)ifnextchar.gobble.